

Raman-scattering investigations in tetragonal tungsten bronze compounds. I. $Ba_2NaNb_5O_{15}$ and related crystals

A. Boudou and J. Sapiel

Centre National d'Etudes des Telecommunications, 92220 Bagneux, France

(Received 30 April 1979)

Raman-scattering experiments have been performed on $Ba_2NaNb_5O_{15}$ crystals between 600 and 1.5 K. All the optical modes at $k=0$ which are Raman active have been systematically investigated. No soft mode has been observed concerning the paraelastic-ferroelastic transition at $T_0 \approx 575$ K. The most obvious effect of this transition is the splitting of the E modes of the quadratic phase into the $B_1(x)$ and $B_2(y)$ modes of the orthorhombic phase. The lowest-frequency $B_2(y)$ line gives rise to a Raman-inactive mode above T_0 . Besides, this line is a feature characteristic of the orthorhombic structure. The evolution of its frequency (which softens markedly on cooling) as well as its intensity (which gives an estimate of the magnitude of the crystal orthorhombicity) is given versus temperature from T_0 to 1.5 K. The investigations are extended to $Ba_{2+x}Na_{1-2x}Nb_5O_{15}$ with respect to the variable x , these solid solutions being studied as single crystals or as polycrystalline ceramics. Substitutions of the cations (Ba by Sr and Na by K) and the Nb atoms by Ta, Ti, and W are also examined in ceramic samples by means of Raman scattering, the study being principally focused on the low-frequency vibrational spectra.

I. INTRODUCTION

The tetragonal tungsten-bronze-type compounds can be grown as large optically homogeneous samples and exhibit high linear electro-optic and second-harmonic coefficients.^{1,2} Besides, as they are free from optic damage, they can be considered as potential materials for devices.

They possess a rather complex structure, the projection of which, in a plane perpendicular to the z axis, is represented on Fig. 1. It can be regarded as consisting of a framework of sharing corner oxygen octahedra,³ forming three, four, and five membered rings in such a way that three types ($A1$, $A2$, and C) of interstitials result, which may receive different metal atoms. The unit cell is then tetragonal, or nearly tetragonal. The general formula is $(A1)_2(A2)_4(C)_4(B1)_2(B2)_8O_{30}$. The oxygen atoms of each octahedron surround an atom which is frequently Nb, Ta, Ti, or W located at B sites. This structure is unstable and most of the tetragonal tungsten bronzes undergo phase transitions versus temperature. We restricted our investigations to alkali-alkaline-earth solid solutions whose prototype is $Ba_2NaNb_5O_{15}$. An important part of our study will be therefore devoted to this crystal. Different cation substitutions in the $A1, A2$ sites as well as replacements of the Nb atoms in the B sites, consistent with the size and charge requirements of the lattice, can be made with attendant variations in physical properties. Moreover, these substitutions can induce modifications of the crystal phases and the transitions critical temperatures.

From a crystallographic point of view, all compounds belonging to this structure have comparable values of the lattice parameters. Indeed⁴

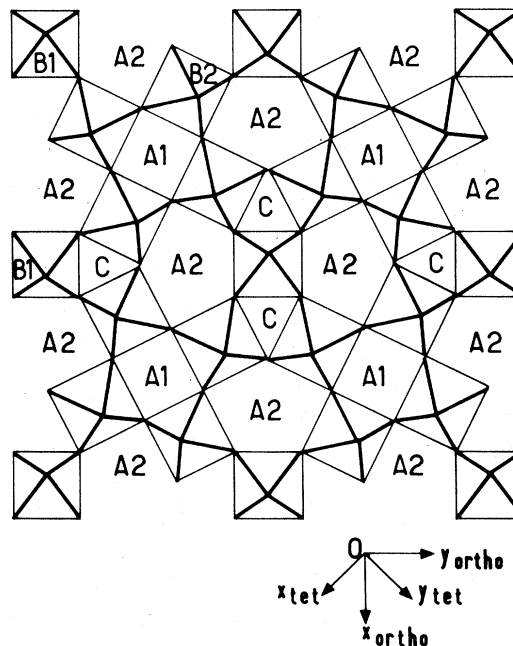


FIG. 1. Tetragonal tungsten-bronze structure (after Ref. 5) with the position of the orthorhombic axes with respect of the quadratic system. The octahedra tilts are represented following the assumption of J. C. Tolédano (Ref. 6).

$a \approx b \approx 12.5 \text{ \AA}$ and $c \approx 4 \text{ \AA}$ (or a multiple) and powder x-ray data exhibit spectra quite similar from one composition to another. One can likewise expect that the vibrational spectra as well as lattice dynamics possess many common characteristics.

As the unit cell of these materials contains a great number of atoms (92 in the orthorhombic phase of $\text{Ba}_2\text{NaNb}_5\text{O}_{15}$) the spectra show many lines which overlap due to disorder broadening. Consequently detailed group factor analysis would be aimless. Only the chief features of the spectra will be pointed out in the text.

In Sec. II, a polarized Raman study on commercially available $\text{Ba}_2\text{NaNb}_5\text{O}_{15}$ crystals is reported, between 600 and 1.5 K. Actually, none of them corresponded exactly to the stoichiometric formula and small variations of compositions which existed from one sample to another, induced marked differences, on cooling the crystals, between the associated low-frequency B_2 spectra.

Following these observations, we have carried out Raman measurements on $\text{Ba}_{2+x}\text{Na}_{1-2x}\text{Nb}_5\text{O}_{15}$ crystals grown in the laboratory, in the range of compositions compatible with both the tetragonal tungsten-bronze structure and single crystals of good optical quality (Sec. III).

In Sec. IV we report Raman measurements on $\text{Ba}_{2+x}\text{Na}_{1-2x}\text{Nb}_5\text{O}_{15}$ compositions in ceramic form, which allow study of a wide range of x values. Besides, as we have recognized a deal of information in the spectra of ceramics on the vibrational modes found in Secs. II and III, we have extended our observations (Sec. V) to other ceramics obtained by substitution, either of the cations, or of the Nb atoms, crystals of such compositions being not available.

The Raman-active lattice vibrational modes in oxygen octahedra compounds generally exhibit high scattering efficiencies, and consequently no sensitivity problem appeared in the spectra, which were detected with a Coderg T 800 triple monochromator ended by a cooled 56 TVP radiotechnique multiplier with a magnetic defocusing and a dc detection. We used a coherent radiation CR4 Ar⁺ laser (5145 and 4880 Å), chiefly on the 5145 Å exciting line; 90° and 180° scattering experiments were performed which allowed many different geometrical configurations required for the polarized Raman study of crystals. In the case of ceramics, which were prepared in compact form, the laser beam was focused onto the surface of the sample by means of a cylindrical lens in order to avoid the large power densities produced by a spherical lens, and the backward scattered light was then analyzed. In addition, an optical filter was introduced in the experimental setup to suppress the spurious incoherent lines of the laser. The spectra were recorded with a spectral resolution comprised between 1 and 2 cm^{-1} .

II. RAMAN SCATTERING IN $\text{Ba}_2\text{NaNb}_5\text{O}_{15}$ CRYSTALS

A. General features of the vibrational spectra

The structure of $\text{Ba}_2\text{NaNb}_5\text{O}_{15}$ has been studied by Jamieson *et al.*⁵ In the general formula the $B1$ and $B2$ sites are fully occupied by Nb, the $A2$ sites by Ba^{2+} and the $A1$ sites by Na^+ cations. Actually in the crystal of Ref. 5 the Ba atoms were in excess and there was a lack of Na with respect to the stoichiometric formula. In addition to the $A2$ sites, the Ba atoms occupied 6,5% of the $A1$ sites though 87% of these sites were occupied by Na. The correct formula was therefore $\text{Ba}_{2+x}\text{Na}_{1-2x}\text{Nb}_5\text{O}_{15}$ with $x = 0.065$. The commercially available crystals which were used in our experiments had also Ba atoms in excess. The proportion of Ba, measured by radiochemical methods was¹⁷ variable from one sample to another ($0.070 < x < 0.087$).

In its highest-temperature phase, above $T_c = 850 \text{ K}$, $\text{Ba}_2\text{NaNb}_5\text{O}_{15}$ belongs to the point group $4/mmm$. Between T_c and T_0 the crystal is tetragonal $4mm$. A spontaneous polarization appears in this phase along the z axis and the crystal is ferroelectric. Below T_0 ($\approx 575 \text{ K}$) it becomes orthorhombic (point group $mm2$) with a doubling of the unit cell⁶ and possesses ferroelectric as well as ferroelastic properties. The procedure to obtain single domain samples is given in Ref. 5.

A Raman study has been undertaken⁷ previously on $\text{Ba}_2\text{NaNb}_5\text{O}_{15}$ crystals, but no effect on the vibrational modes was seen, due to the ferroelastic transition at T_0 . Besides several characteristics of the spectra specially the softening of the B modes on cooling the crystal,⁸ which are reported in our study, were not noted in Ref. 7.

In tetragonal tungsten-bronze-type crystals one can distinguish to a first approximation between internal modes of the oxygen octahedra and external modes due to the lattice vibrations involving cations motions with respect to the octahedra framework.⁹ These external modes are situated in the low-frequency part of the Raman spectra and depend on the nature of the cations. Two sets of lines situated around 280 and 650 cm^{-1} of symmetry $A_1(z)$ have been already identified as internal modes of NbO_3 octahedra.¹⁰

At room temperature the crystal is orthorhombic. All the optical modes are Raman active and the Raman tensors have the well-known form¹¹

$$\begin{matrix} A_1(z) & A_2 & B_1(x) & B_2(y) \\ \left(\begin{matrix} a & & & \\ & b & & \\ & & c & \end{matrix} \right), & \left(\begin{matrix} d & \\ & d \end{matrix} \right), & \left(\begin{matrix} e \\ & e \end{matrix} \right), & \left(\begin{matrix} & & & \\ & & & f \\ & & & \end{matrix} \right). \end{matrix}$$

$A_1(z)$, $B_1(x)$, and $B_2(y)$ are polar modes and can

TABLE I. Correspondence between the symmetries of the normal modes in the high-temperature ($4mm$) and low-temperature ($mm2$) phases of $Ba_2NaNb_5O_{15}$.

$4mm$		$mm2$
$A_1(z)$	\leftrightarrow	$A_1(z)$
A_2	\leftrightarrow	A_2
B_2	\leftrightarrow	$A_1(z)$
B_1	\leftrightarrow	A_2
E	\leftrightarrow	$B_1(x) + B_2(y)$

give rise to longitudinal and transverse components.¹² Throughout this work, the notation x, y, z will refer to the principal axes of the orthorhombic phase. Above T_0 , the crystal is quadratic $4mm$. The Raman tensors are

$$\begin{array}{c}
 A_1(z) \quad B_1 \quad B_2 \quad E(X) \quad E(Y) \\
 \left(\begin{array}{c} a \\ a \\ b \end{array} \right), \left(\begin{array}{c} c \\ -c \end{array} \right), \left(\begin{array}{c} d \\ d \end{array} \right), \left(\begin{array}{c} e \\ e \end{array} \right), \left(\begin{array}{c} e \\ e \end{array} \right)
 \end{array}$$

In Table I is given the correspondence between the modes of the point group $4mm$ and those of the point group $mm2$ (the fact that the axes X and Y of the tetragonal phase are rotated through 45° around the z axis with respect to the axes x and y of the orthorhombic phase, is taken into account).

We give (Fig. 2) between 1.5 and 600 K the spectra relative to internal modes of the octahedra NbO_3 , which are particularly intense in $x(zz)y$ geometrical

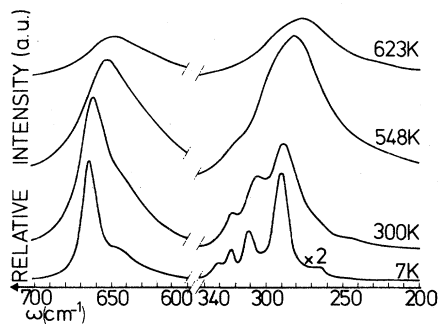


FIG. 2. Octahedra internal modes, vs temperature in $Ba_2NaNb_5O_{15}$. Two sets of strong Raman lines around 300 and 650 cm^{-1} are observed for instance at $x(zz)y$ scattering geometry corresponding to TO $A_1(z)$ modes. The intensities of the set situated around 300 cm^{-1} have been multiplied by a factor of 2, at 7 K, by a scale change of the electric detection. Besides, the relative intensities of the two bands at 650 and 300 cm^{-1} are respected.

configurations and correspond to the TO $A_1(z)$ modes. Besides, a line which appears at 870 cm^{-1} in all the tetragonal tungsten-bronze composition has been identified by us as the highest-frequency LO $A_1(z)$ mode associated to internal modes of the oxygen octahedra. This line of medium intensity is visible in $z(xx)\bar{z}$, $z(yy)\bar{z}$ and disappears for scattering geometries corresponding to TO $A_1(z)$ modes like $x(zz)\bar{x}$ and $y(zz)\bar{y}$.

We have reported (Figs. 3–5) the low-frequency part of the spectra corresponding to geometrical configurations associated to $A_1(z)$, A_2 , $B_1(x)$, and $B_2(y)$ symmetries of the orthorhombic phase as well as their evolution versus temperature between 1.5 and 600 K, the paraelectric-ferroelectric transition which occurs at 850 K being out of the purpose of this study. It can be noted that the spectra corresponding to $A_1(z)$ and A_2 are about 15 times less intense than those corresponding to $B_1(x)$ and $B_2(y)$.

It can be noted in Figs. 3–5 that no soft mode appears in the phase $mm2$ when the critical temperature is approached from below. Beyond the spectra the most interesting are those corresponding to the $B_1(x)$ and $B_2(y)$ mode. In addition to their high intensity, the lines belonging to these symmetries are relatively narrow, at least if one compares them to the structureless spectra A_1 of Fig. 3. Therefore particular attention will be devoted to these B modes.

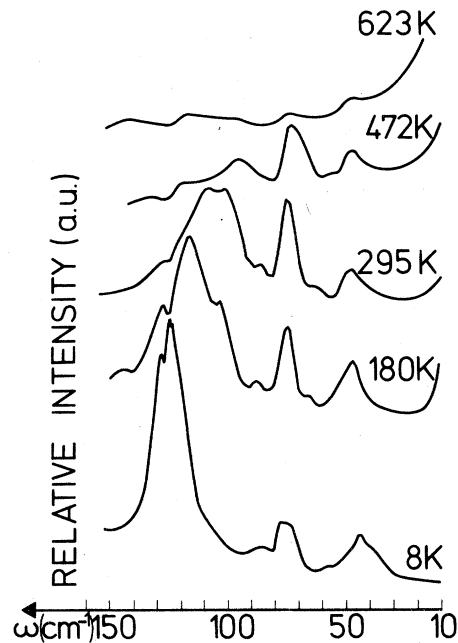


FIG. 3. Low-frequency part of the spectra corresponding to TO $A_1(z)$ modes, observed at the $x(zz)y$ scattering geometry and vs temperature in $Ba_2NaNb_5O_{15}$.

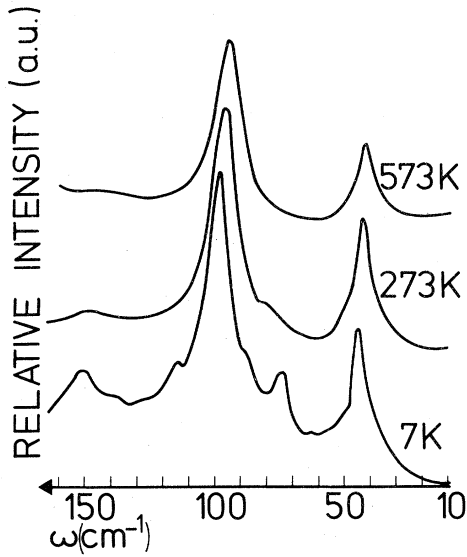


FIG. 4. Low-frequency part of the A_2 modes vs temperature in $Ba_2NaNb_5O_{15}$.

B. Influence of the transition at T_0 on the low-frequency B modes dynamical behavior ($300 < T < 600$ K)

It can be noted from Table I that each two-dimensional E mode belonging to $4mm$ split into a couple of one-dimensional modes $B_1(x)$ and $B_2(y)$ in $mm2$. One can expect that these B_1 and B_2 modes issued from the same E mode have nearly the same frequency. Therefore, it is not surprising that the $B_1(x)$ and $B_2(y)$ spectra in the orthorhombic phase, present many similarities. They can be respectively observed in the geometrical configurations $z(xz)y$ and $z(yz)x$ which both correspond to TO lattice vibrations. When the temperature is raised from 300 K to T_0 , the differences between the two spectra grow smaller and smaller till they merge into a single E spectrum (Fig. 5) at T_0 . Above T_0 the spectra corresponding to E apparently undergo no modifications with temperature.

Let us consider the lowest-frequency TO $B_2(y)$ line situated at 32 cm^{-1} at room temperature, which is visible in $z(yz)x$ scattering geometry. There is no corresponding $B_1(x)$ line in $z(xz)y$. Besides, the intensity of this $B_2(y)$ mode decreases regularly from 300 K to T_0 and cancels above T_0 . The Raman inactivity in the $4mm$ phase is probably due to the fact that this mode is shifted above T_0 , to a point of the Brillouin zone, other than the center. As x-ray measurements have evidenced a doubling⁶ of the lattice parameter c at T_0 , the mode $B_2(y)$ under consideration would therefore be situated in the boundary of the Brillouin zone (Z point) in the quadratic phase.

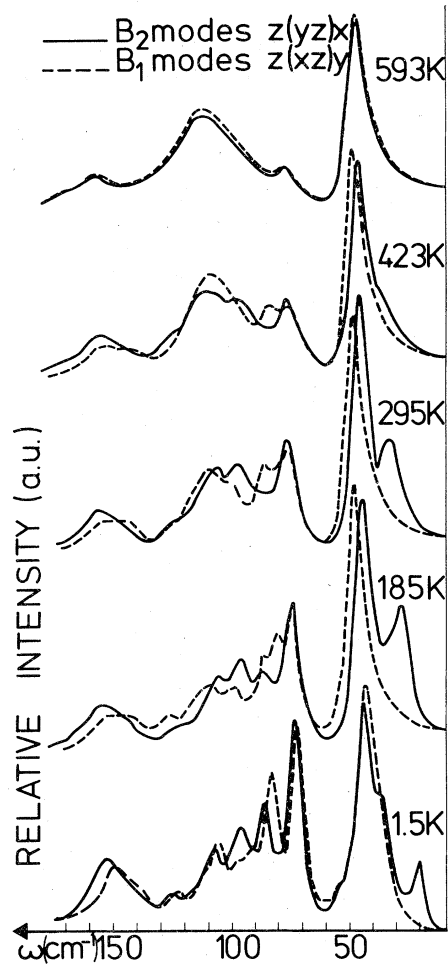


FIG. 5. TO $B_1(x)$ and $B_2(y)$ modes of the orthorhombic phase in $Ba_2NaNb_5O_{15}$ observed respectively at $z(xz)y$ and $z(yz)x$ scattering geometries. Above $T_0 \approx 575$ K the spectra merge into the quadratic E spectrum and the lowest-energy $B_2(y)$ mode (called the characteristic mode in the text) disappears.

It can be noted that this B_2 mode hardens when the temperature of transition T_0 is approached from below. Besides, its presence is characteristic of the existence of the orthorhombic phase in the tetragonal tungsten-bronze crystals. That means that it appears in the orthorhombic phase and disappears in the high-temperature tetragonal phase, not only in $Ba_2NaNb_5O_{15}$ crystals, but also in all the related solid solutions we have investigated by means of Raman scattering (Sec. V).

C. Softening of the B modes on cooling the crystal

There is a continuous decrease of energy for several low-frequency B modes when the temperature

is lowered from T_0 to 1.5 K. A particularly important softening on cooling the crystal is associated to the characteristic TO $B_2(y)$ line pointed out in Sec. II B. Indeed, from 450 to 1.5 K its frequency ω shifts from 36 to 19 cm^{-1} , though, in this temperature range, its width Γ varies from 9 to 5 cm^{-1} . As the ratio Γ/ω is smaller than 0.3 in this temperature range, this mode can be considered as underdamped. Its frequency as well as the square of its frequency have been determined versus temperature for $\text{Ba}_2\text{NaNb}_5\text{O}_{15}$ crystals of different sources. The frequency square varies linearly with temperature (Fig. 6). The representative line has a slope equal to $2 \pm 0.1 \text{ cm}^{-2}/\text{K}$. Extrapolation of the line $\omega^2 = f(T)$ in Fig. 7 gives a cancellation of the energy for a negative temperature $T_c \approx -170 \text{ K}$. Above 450 K, the proximity of the 47 cm^{-1} line in conjunction with the fact that the intensity decreases, reduce the possibility of following the variations with sufficient accuracy. Besides, spurious light coming from the Rayleigh line increases markedly with temperature and reduces the contrast. Additional softening (of the order of a few cm^{-1}) of several other low-frequency B modes have been observed on cooling. But the frequency shifts are about 10 times smaller than that of the characteristic mode.

Let us examine the connection between the frequencies of the vibrational modes and the dielectric constant variations through the generalized Lyddane-Sachs-Teller relation¹³ which is given by

$$\prod_{i=1}^n \frac{\omega_L^2(\alpha)}{\omega_T^2(\alpha)} = \frac{\epsilon_{\alpha\alpha}^0}{\epsilon_{\alpha\alpha}^\infty}, \quad (1)$$

where α is the direction of a principal axis, ω_L and ω_T are the frequencies of the n longitudinal and transverse modes polarized along α . ϵ^0 and ϵ^∞ are, respectively, the static and high-frequency dielectric constants. One obtains from the derivative of Eq. (1) with respect to temperature T

$$\frac{1}{\epsilon_{\alpha\alpha}^0} \frac{\Delta \epsilon_{\alpha\alpha}^0}{\Delta T} \approx \sum_{i=1}^n \frac{2}{\omega_L} \frac{\Delta \omega_L}{\Delta T} - \sum_{i=1}^n \frac{2}{\omega_T} \frac{\Delta \omega_T}{\Delta T}. \quad (2)$$

For a precise evaluation of the first member of Eq. (2), the knowledge is needed of at least the longitudi-

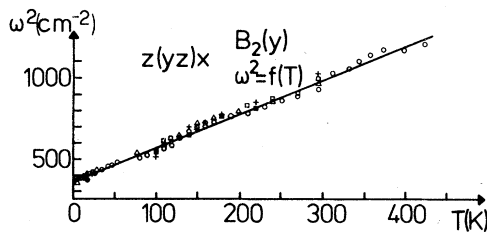


FIG. 6. Square frequency dependence of the characteristic mode, in commercially available $\text{Ba}_2\text{NaNb}_5\text{O}_{15}$ crystals of different sources showing a linear behavior in the range 450–1.5 K.

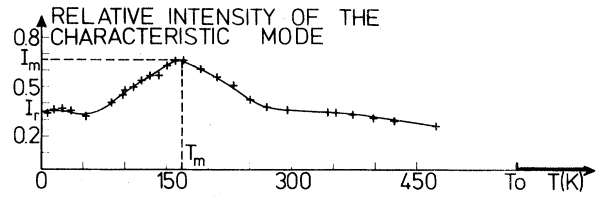


FIG. 7. Relative peak amplitude I of the characteristic line (the reference taken is the intensity of the B_2 line situated at 45 cm^{-1}) for one of the $\text{Ba}_{2+x}\text{Na}_{1-2x}\text{Nb}_5\text{O}_{15}$ crystals ($x=0.087$). For $450 \text{ K} < T < T_0$, the possibility of following the variations of the characteristic mode with sufficient accuracy is considerably reduced. Above T_0 , this mode is Raman inactive.

nal vibrational frequencies which are associated to the TO B modes which soften with temperature. One notes that if TO B modes are seen in several configurations, like $z(xz)y$ or $y(xz)\bar{y}$ for the $B_1(x)$ modes, and $z(yz)x$ or $x(yz)\bar{x}$ for $B_2(y)$ modes, no experimental arrangement allows the observations of pure LO B modes. On the other hand on performing measurements in scattering geometries like $x(yz)y$ and $y(xz)x$ corresponding to oblique B modes, we have not been able to separate at any temperature the longitudinal components from the transverse ones. It is likely that the LO-TO splitting of the low-frequency B modes remains weak at every temperature.

Schneck *et al.*^{14,15} have observed an increase of the dielectric constant when the temperature is lowered down to 1.5 K, which accounts qualitatively for the softening of the B modes. Actually the variations of the dielectric constant are less important than one can expect from the variations of the only characteristic $B_2(y)$ mode. It is therefore likely that the variations of the longitudinal modes partially compensate those of the transverse modes as can be seen through Eq. (2).

It can be seen from Fig. 6 that the frequencies of the lowest-frequency $B_2(y)$ mode does not vary from one sample to another. The same is not the case with its intensity as we shall see (Sec. IID).

D. Temperature dependence of the intensity of the characteristic $B_2(y)$ mode

We have pointed out that the intensity of the lowest-frequency TO $B_2(y)$ mode (which we shall henceforth call, for the sake of simplicity, the characteristic mode) which is zero above T_0 , increases when the crystal is cooled below T_0 . This is indeed not surprising if one remembers that this mode is characteristic of the orthorhombic structure. But what is valuable to note is that this increment on cooling takes place during a range of about 400 K and then

the peak amplitude of the characteristic mode undergoes a noticeable decrease till 1.5 K. Such variations are represented for one of the crystals ($x = 0.087$) on Fig. 7. For $T \approx 10$ K the peak amplitude achieves its minimum I_r . Besides, when observed between polarizers, the contrast between domains of $\text{Ba}_2\text{NaNb}_5\text{O}_{15}$, which is enhanced, reaches a maximum and then decreases again on cooling, seems to be a consequence of the same phenomenon. Other experimenters,^{14,15} have reported that the birefringence as well as the difference $b - a$ of the lattice parameters in the x - y plane undergo comparable variations which express an increase of the orthorhombicity during a range of temperature of the same order, followed by a notable decrease. These authors interpreted their results as the consequence of a reversed transition $mm2 \rightarrow 4mm$, at 110 K and a cooperative pseudo-Jahn-Teller mechanism was proposed¹⁶ to explain the succession of transitions in $\text{Ba}_2\text{NaNb}_5\text{O}_{15}$. Yet, according to our measurements, the persistence of the $B_2(y)$ mode till 1.5 K shows that the return to a tetragonal phase on cooling is rather a tendency than a reality. We observed that this tendency was more or less important according to the investigated sample. Such crystal-dependent behavior at low temperatures has been already pointed out¹⁵ through dielectric and birefringence properties. We have consequently performed a set of experiments in order to determine through the Raman spectra the influence of the composition on the decrease of the orthorhombicity at low temperatures, in the compositions $\text{Ba}_{2+x}\text{Na}_{1-2x}\text{Nb}_5\text{O}_{15}$ where the ratio of the cations Ba^{2+} and Na^+ is made to vary. In the same compositions we have been also able to appreciate the evolution of the temperature T_0 of the paraelastic-ferroelastic transition.

III. RAMAN SCATTERING IN $\text{Ba}_{2+x}\text{Na}_{1-2x}\text{Nb}_5\text{O}_{15}$ SINGLE CRYSTALS

We have already pointed out that the $\text{Ba}_2\text{NaNb}_5\text{O}_{15}$ crystals are actually solid solutions $\text{Ba}_{2+x}\text{Na}_{1-2x}\text{Nb}_5\text{O}_{15}$ with small positive values of x . This section differs from Sec. II only in the sense that the deviation from stoichiometry of the crystals are induced instead of being accidental. We have tried to explore the largest range of values of x compatible with the tetragonal tungsten-bronze structure, and with samples of rather good optical qualities in order to perform polarized Raman study.

The following Raman investigations belong to a comprehensive set of studies, specially including crystal growth, x-rays, and radiochemical analyses, birefringence and dielectric measurements.¹⁷ It has been noted by radiochemical techniques, that the crystals which were grown by the Czochralski growth procedure, systematically contained less Na than the

starting melt, resulting from a Na segregation phenomenon during the crystallization.¹⁸ The results of our Raman investigations can be summarized as follows:

- (i) The transition temperature T_0 decreases with x [Fig. 8(a)]. (ii) The maximum I_m of the characteris-

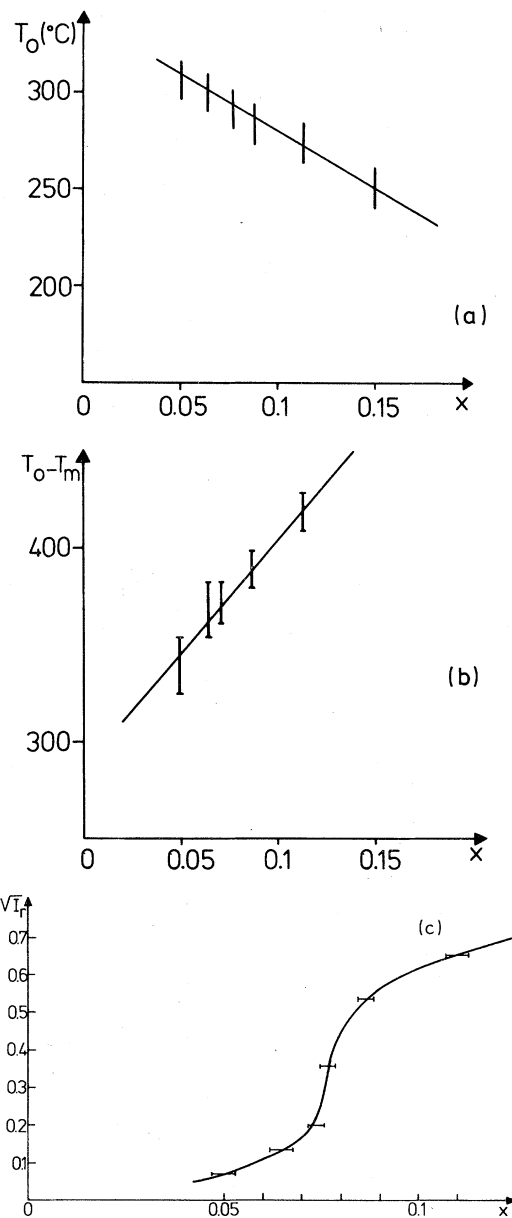


FIG. 8. (a) Variations of the transition temperature T_0 for different concentrations, x , in single crystals $\text{Ba}_{2+x}\text{Na}_{1-2x}\text{Nb}_5\text{O}_{15}$. (b) $T_0 - T_m$ vs x , T_m being the temperature at which the intensity of the characteristic mode reaches its maximum I_m . (c) Square root $\sqrt{I_r}$ of the residual intensity of the characteristic mode vs x ($T \approx 10$ K). For $x < 0.075$ the intensity becomes very weak. No crystal has been able to be grown for $x < 0.05$.

tic mode is reached at a temperature T_m , such as $T_0 - T_m$ increases with x [Fig. 8(b)]. (iii) The minimum value of the intensity I_r of the characteristic line at low temperature (≈ 10 K) becomes smaller with decreasing values of x ; for values of $x < 0.075$ the intensity I_r of the characteristic line becomes very weak. Figure 8(c) and the differences between $B_2(y)$ and $B_1(x)$ spectra become very small. Measurements on the birefringence $|n_y - n_x|$ undertaken on the same samples, have shown that this physical quantity undergoes the same kind of variations versus temperature and concentration x as the intensity of the characteristic line.¹⁷ Concerning negative values of x which correspond to an excess of Na, no crystal with good enough optical quality could be obtained from the original melt. In order to study compositions with an excess of Na we have been led to investigate ceramics, which, as they result from solid phase chemical reactions, are expected not to introduce Na segregation phenomenon.

It is worth noting the presence at low temperatures of an additional line of symmetry $B_2(y)$, situated at 36 ± 1 cm^{-1} , which appears in the vicinity of T_m and whose origin is not yet elucidated (see Fig. 5).

IV. INTEREST OF $\text{Ba}_{2+x}\text{Na}_{1-2x}\text{Nb}_5\text{O}_{15}$ COMPOSITIONS IN CERAMIC FORM

The investigated ceramics were prepared in the laboratory¹⁹ from mixture of pentoxides of Nb and carbonates of Ba and Na in suitable proportions. These mixtures were grinded pelletized and fired at 30 to 100 K below the appropriate solid temperature for 17 h. The procedure was repeated several times to ensure complete reaction and the final product had a compact disk form after a pressure of the order of 200 kg/cm^2 has been applied for a short time.

Burns and Scott²⁰ have shown that Raman scattering from polycrystalline solids contains essential features of single-crystal studies. Besides, the advantage of ceramics seem evident for compounds for which single crystals are not available, as $\text{Ba}_{2+x}\text{Na}_{1-2x}\text{Nb}_5\text{O}_{15}$ containing an excess of Na ($x < 0$). Another interesting aspect of ceramics is that the composition is more easily controllable, though for single-crystal growth in liquid phase, the proportion of the constitutive elements can evolve and the final product is often different than expected.

The first step in a Raman study of ceramics is to compare a spectrum obtained from a ceramic to the polarized spectra corresponding to a crystal of the same composition. The spectrum of a ceramic is evidently the superposition of all the spectra corresponding to the different Raman active modes which propagate in all directions in the crystal. The polarized Raman study of Sec. II A allowed us to establish that

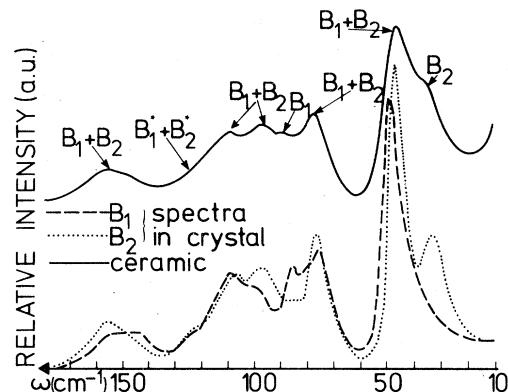


FIG. 9. Identification of the symmetries of the modes by comparison of a ceramic and a single-crystal spectra in $\text{Ba}_2\text{NaNb}_5\text{O}_{15}$ (room temperature). The modes B_1^* , B_2^* are seen only at low temperatures (< 150 K) on ceramics.

below 180 cm^{-1} the B modes were about 15 times more intense than the A modes in $\text{Ba}_2\text{NaNb}_5\text{O}_{15}$.

One can therefore expect that the spectra of a ceramic is essentially a superposition of B modes in this frequency range. We have reported on Fig. 9 at room temperature, the spectra $B_1(x)$ and $B_2(y)$ of the crystal as well as the spectrum obtained from a ceramic of the same composition. It is thus easy to identify the Raman lines of the ceramic. The characteristic $B_2(y)$ mode appears as a shoulder of the 47 cm^{-1} line. We have investigated ceramics of $\text{Ba}_{2+x}\text{Na}_{1-2x}\text{Nb}_5\text{O}_{15}$ formula in the range $-0.12 < x < +0.22$ where it has been established that the tungsten-bronze structure exists.²¹ When x varies between these limits, there are neither appearance of new lines nor disappearance of the existing lines in the Raman spectra of ceramics at room temperature. The only effect is the variation of the relative intensities of the lines due to the difference between the temperature of the ceramic and the temperature T_0 of the corresponding transition. Besides, the information on the characteristic mode found on crystals are contained in the ceramic spectra; i.e., we have checked that, when the temperature is lowered: the frequency of the characteristic mode softens, and its intensity increases, reaches a maximum and then decreases again. Besides, the more the composition contains Na^+ cations and the smaller is the intensity I_r of the characteristic modes at low temperatures (~ 10 K), in conformity with the results obtained from crystals.

V. EFFECTS OF ATOMIC SUBSTITUTIONS ON THE VIBRATIONAL SPECTRA

We have proceeded to substitute two kinds of atoms in $\text{Ba}_2\text{NaNb}_5\text{O}_{15}$: the replacement of the ca-

tions (Ba by Sr, Na by K) and partial or total substitutions of the Nb at the center of the octahedra by Ta, Ti, or W. The introduction of Ti and W atoms, to which are associated respectively the charge 4+ and 6+, as substitutes of Nb whose charge is 5+, must be accompanied by a variation of the number of cations Ba^{2+} and Na^+ in order to preserve the electrical neutrality. The corresponding formulas are, respectively, $Ba_{2+x}Na_{1-x}Ti_xNb_{5-x}O_{15}$ and $Ba_{2-x}Na_{1+x}Nb_{5-x}W_xO_{15}$. The total number of cations is equal to the total number of sites A1 and A2 which are therefore completely filled.

All the investigated compounds were prepared in ceramic form by a method similar to that described in Ref. 19.

The set of Raman lines around 280, 660, and 850 cm^{-1} which correspond to the octahedra internal movements can always be identified in the different ceramics. Below 200 cm^{-1} the spectra, according to our observations, are strongly dependent on the couple of alkali-alkaline-earth cations present in the formulas, but are scarcely dependent on the atoms situated at the center of the octahedra, whose interactions with the cations are weak. On the other hand the relative intensities of the lines vary from one

spectrum to another, and this originates principally from the variations of T_0 with the compositions, as already observed on $Ba_{2+x}Na_{1-2x}Nb_5O_{15}$ solid solutions. It is worth noting that the spectra of most of the investigated ceramics are not less defined than that of the prototype $Ba_2NaNb_5O_{15}$. Yet $Sr_2NaNb_5O_{15}$ gives relatively smeared out spectra and this is the consequence of a greater amount of disorder due probably to very comparable sizes of Na^+ and Sr^+ cations (the ionic radii are, respectively, 0.95 and 1.13 Å) which can indifferently fill the sites A1 and A2.

In Table II column 4 are given the results of our Raman investigations, between 300 and 1.5 K, on $Ba_2NaNb_5O_{15}$ related compounds, concerning essentially the characteristic mode and its softening. The transition temperatures T_0 associated to the different compositions and the methods used for their determinations are indicated in columns 2 and 3. The relation between the presence of the characteristic mode and the orthorhombicity clearly appears on Table II.

It is worth pointing out that Raman scattering on ceramics of such compositions allows a quick detection of the orthorhombicity when powder x-ray data are generally unable to give such an information,

TABLE II. Results of the Raman investigations on $Ba_2NaNb_5O_{15}$ related compounds, between 1.5 and 300 K.

Compositions	Transition temperature T_0 (K)	Determination method of T_0	Our Raman observations
$Ba_{2.25}Na_{0.75}Nb_{4.75}Ti_{0.25}O_{15}$	470	Birefringence and dielectric measurements ^a	Observation of a small characteristic mode (the orthorhombicity ^a being weak) which softens on cooling.
$Ba_{2.55}Na_{0.45}Nb_{4.45}Ti_{0.55}O_{15}$	310		
$Ba_3TiNb_4O_{15}$	No observation of a ferroelastic transition		No characteristic mode
$Ba_{2-x}Na_{1+x}Nb_{5-x}W_xO_{15}$	580	Dielectric measurements ^b	Very clear spectra which show the presence of the characteristic mode as well as its frequency dependence vs temperature
$Sr_2NaNb_5O_{15}$	455	Dielectric measurements ^c	Relatively smeared out spectra
$Ba_2KNb_5O_{15}$	No ferroelastic transition	No ferroelastic domain structure was detected ^d	No characteristic mode
$Ba_2NaTa_5O_{15}$	No transition at all (ferroelectric or ferroelastic) in the range $77 < T < 900$ K	Dielectric measurements ^e	No characteristic mode till 77 K. Below 40 K, emergency of this mode, indicating a ferroelastic transition

^aT. Ikeda and I. Fujimura, Jpn. J. Appl. Phys. **13**, 57 (1974).

^bB. Elouadi, J. M. Reau, and J. Ravez, Bull. Soc. Chim. France **3-4**, 467 (1975).

^cL. G. Van Uitert, J. J. Rubin, W. H. Grodkiewicz, and W. A. Bonner, Mater. Res. Bull. **4**, 63 (1969).

^dG. Burns, E. A. Giess, D. F. O'Kane, B. A. Scott, and A. W. Smith, J. Appl. Phys. **40**, 901(c) (1969).

^eJ. P. Chaminade, A. Perron, J. Ravez, and P. Hagenmuller, Bull. Soc. Chim. France **10**, 3751 (1972).

since the difference $b - a$ of the lattice parameters is too weak.

VI. DISCUSSION AND CONCLUSION

One of the aims of this study is to point out the effect of the paraelastic-ferroelastic transition at T_0 on the vibrational modes. Actually this is the first time that the symmetry change at T_0 is shown by means of Raman scattering in $\text{Ba}_2\text{NaNb}_5\text{O}_{15}$ or related compounds. The transition occurs without the appearance of any mode softening (in the high-temperature phase as well as the low-temperature phase), which could establish the displacive character of the transition. The splitting of the E modes of the quadratic phase into $B_1(x)$ and $B_2(y)$ modes in the orthorhombic phase, is the most visible effect of the transition on the Raman spectra. Beyond the optical modes, the one which carries the maximum information is the lowest-frequency $B_2(y)$ mode. It appears or disappears according to the symmetry of the phase under consideration. Above T_0 it is shifted to a point of the Brillouin zone other than the center, and is therefore Raman inactive. Moreover its intensity gives a qualitative estimation of the magnitude of the orthorhombicity.

This characteristic mode softens markedly when the crystal is cooled from T_0 to 1.5 K. Its intensity at 10 K in $\text{Ba}_{2+x}\text{Na}_{1-2x}\text{Nb}_5\text{O}_{15}$ varies with x . Higher the proportion of Na^+ cations in the solid solution, less is the residual intensity of the characteristic mode at 10 K. Besides, the symmetry as well as the softening of this mode have been confirmed by infrared absorp-

tion measurements.²² Some questions arise from these sets of results. Particularly, one can wonder if it is possible to induce a transition around this temperature by applying an external excitation (electric field or induced stress), and to what phase the crystal evolves in these conditions. We have also pointed out certain modifications of the spectra occurring near the temperature T_m corresponding to the maximum of the characteristic mode intensity. More experimental data is needed (Brillouin, neutrons scattering, infrared absorption) to interpret details of the whole set of Raman observations collected in this paper, specially in terms of phase transition theories.^{23,24} Nevertheless, in the meantime, we have extended some of the results (particularly those concerning the characteristic mode and its softening) obtained on $\text{Ba}_{1+x}\text{Na}_{1-2x}\text{Nb}_5\text{O}_{15}$, to other compounds obtained by substitutions of either the cations, or the atom situated at the center of the oxygen octahedra.

ACKNOWLEDGMENTS

The authors are particularly grateful to X. Gerbault and A. Hadni for communicating to them their first infrared results. This study is greatly indebted to B. Joukoff who has grown all the crystals and kindly informed us about the crystal growth, and to R. Mellet for the radiochemical analysis. It is also a pleasure to acknowledge D. Morin and L. Dugrand for the ceramics preparation. The authors would like to thank J. Jerphagnon for constant encouragement throughout this study and C. Sebenne for a careful reading of the manuscript and for comments.

-
- ¹J. E. Geusic, H. J. Levinstein, J. J. Rubin, S. Singh, and L. G. Van Uitert, *Appl. Phys. Lett.* **11**, 269 (1967).
²S. Singh, D. A. Draegert, and J. E. Geusic, *Phys. Rev. B* **2**, 2709 (1970).
³P. B. Jamieson, S. C. Abrahams, and J. L. Bernstein, *J. Chem. Phys.* **48**, 5048 (1968).
⁴E. A. Giess, B. A. Scott, G. Burns, D. F. O'Kane, and A. Segmüller, *J. Am. Ceram. Soc.* **52**, 276 (1969).
⁵P. B. Jamieson, S. C. Abrahams, and J. L. Bernstein, *J. Chem. Phys.* **50**, 4352 (1969).
⁶J. Burgeat and J. C. Tolédano, *Solid State Commun.* **20**, 281 (1976); J. C. Tolédano, *Phys. Rev. B* **12**, 943 (1975).
⁷L. C. Bobb, J. Dahl, I. Lefkowitz, and L. Muldower, *Ferroelectrics* **1**, 247 (1970); L. C. Bobb, I. Lefkowitz, and L. Muldower, *Ferroelectrics* **2**, 217 (1971).
⁸J. Sapriel and D. Morin, in *Proceedings of the International Conference on Lattice Dynamics, Paris, 1977*, edited by Balkanski (Flammarion, Paris, 1978), p. 450; J. Sapriel and A. Boudou, *Ferroelectrics* **21**, 323 (1978).
⁹S. D. Ross, *J. Phys. C* **3**, 1785 (1970).
¹⁰G. Burns, J. D. Axe, and D. F. O'Kane, *Solid State Commun.* **7**, 933 (1969).
¹¹R. Loudon, *Adv. Phys.* **13**, 423 (1964).
¹²H. Poulet and J. P. Mathieu, *Spectres de vibration et symétrie des cristaux* (Gordon and Breach, New York, 1970).
¹³W. Cochran and R. A. Cowley, *J. Phys. Chem. Solids* **23**, 447 (1962).
¹⁴J. Schneck, J. Primot, R. Von Der Mühl, and J. Ravez, *Solid State Commun.* **21**, 57 (1977).
¹⁵J. Schneck and D. Paquet, *Ferroelectrics* **21**, 577 (1978).
¹⁶D. Paquet, *J. Chem. Phys.* **66**, 886 (1977).
¹⁷J. Schneck, B. Joukoff, R. Mellet, and J. Burgeat (unpublished).
¹⁸K. G. Barraclough, I. R. Harris, B. Cockayne, J. G. Plant, and A. W. Vere, *J. Mater. Sci.* **5**, 389 (1970).
¹⁹D. Morin, J. P. Colin, G. Le Roux, L. Pateau, and J. C. Tolédano, *Mater. Res. Bull.* **8**, 1089 (1973).
²⁰G. Burns and B. A. Scott, *Phys. Rev. Lett.* **25**, 1191 (1970).
²¹B. A. Scott, E. A. Giess, and D. F. O'Kane, *Mater. Res. Bull.* **4**, 107 (1969).
²²X. Gerbault and A. Hadni (private communication).
²³L. D. Landau and E. M. Lifschitz, *Statistical Physics* (Addison Wesley, Reading, Mass., 1958).
²⁴J. F. Scott, *Rev. Mod. Phys.* **46**, 83 (1974).